. SCUOLA INTERNAZIONALE SUPERIORE DI STUDI AVANZATI

SISSA Digital Library

Topological gap opening without symmetry breaking from dynamical quantum correlations

Original
Topological gap opening without symmetry breaking from dynamical quantum correlations / Paoletti, F., Fanfarillo, L., Capone, M., Amaricci, A.. - In: PHYSICAL REVIEW. B. - ISSN 2469-9950. - 109:7(2024), pp. 1-6. [10.1103/PhysRevB.109.075148]

Availability:
This version is available at: 20.500.11767/137450 since: 2024-03-29T19:52:38Z

Publisher:

Published
DOI:10.1103/PhysRevB.109.075148

Terms of use:

Testo definito dall'ateneo relativo alle clausole di concessione d'uso

Publisher copyright

note finali coverpage

(Article begins on next page)

09 September 2026

arXiv:2311.10024v1 [cond-mat.str-el] 16 Nov 2023

Topological Gap Opening without Symmetry Breaking from Dynamical Quantum Correlations

F. Paoletti,[1] L. Fanfarillo,[2,1] M. Capone,[1,3] and A. Amaricci[3]

[1] *International School for Advanced Studies (SISSA), via Bonomea 265, 34136 Trieste, Italy*
[2] *CNR-ISC, Via dei Taurini, Rome, Italy*
[3] *CNR-IOM, Istituto Officina dei Materiali, Consiglio Nazionale delle Ricerche, Via Bonomea 265, 34136 Trieste, Italy*

Topological phase transitions are typically associated with the formation of gapless states. Spontaneous symmetry breaking can lead to a gap opening thereby obliterating the topological nature of the system. Here we highlight a completely different destiny for a topological transition in presence of interaction. Solving a Bernevig-Hughes-Zhang model with local interaction, we show that dynamical quantum fluctuations can lead to the opening of a gap without any symmetry breaking. As we vary the interaction and the bare mass of the model, the continuous gapless topological transition turns into a first-order one, associated with the presence of massive Dirac fermion at the transition point showing a Gross-Neveu critical behaviour near the quantum critical endpoint. We identify the gap opening as a condensed matter analog of the Coleman-Weinberg mechanism of mass generation.

The discovery of symmetry protected topological phases of matter [1–8] has enriched the landscape of phase transitions beyond the conventional Landau paradigm of the symmetry-breaking [9, 10]. In presence of a given symmetry the possible electronic band structures of an insulator can be divided into distinct equivalence classes, which can only be connected through the continuous closure of the energy gap from both sides of the transition through a topological quantum phase transition (TQPT). The corresponding formation of symmetry-protected massless Dirac fermions at the transition is a distinctive feature of the topological insulators [11–15].

The presence of interactions can change the above scenario and a gapped state can appear also at the transition. The standard phenomenology for this to occur requires a spontaneous symmetry breaking (SSB) [4, 16–20]. Indeed, breaking a continuous symmetry opens a gap in the energy spectrum or, equivalently, gives a finite mass for the Dirac electrons which is understood in terms of the Anderson-Higgs mechanism. Clearly, a SSB can lead to break any of the symmetry protecting the topological state, thus leaving behind a topologically trivial long-range ordered phase. A similar scenario can be described within a static mean-field picture in the channel where SSB takes place.

A great deal of attention has been recently drawn in different fields [21–23] to novel possible mechanisms of spontaneous mass generation which preserve the symmetry, beyond the conventional SSB description. Here we show that such process describes the gap opening for Dirac electrons at the boundary of a topological insulator. More concretely, we address the question whether or not electron-electron interactions can drive the formation of a spontaneous mass for the otherwise gapless electrons at a topological transition. The lack of a gap closing at the TQPT is expected to change the character of the transition which becomes necessarily discontinuous despite the symmetries protecting the topological phase are preserved.

For the sake of definiteness we consider a two-dimensional Bernevig-Hughes-Zhang (BHZ) model augmented via the inclusion of local electron-electron interactions that preserve some symmetries of the model. Without interactions, this model features a TQPT through the formation of a gapless state. The control parameter of the transition is the energy splitting between two electronic orbitals playing the role of a mass term. As a consequence the difference in the occupation of the orbitals, or orbital polarization, is expected to assume a prominent role. Since the orbital symmetry is broken by the mass term, the concept of SSB does not apply to the TQPT. Within a mean-field theory, the interactions simply dress the mass term, shifting the topological transition without changing its nature with respect to the non-interacting limit.

In this work we go beyond mean-field using a variational approach including quantum fluctuations not only of the orbital polarization, but also in the other particle-hole channels. We demonstrate a new scenario in which a gap opens at the TQPT without breaking any of the symmetries of the model. We show explicitly that the quantum fluctuations in the different channels make the TQPT discontinuous for sufficiently large interactions [24, 25]. The first-order line ends in a critical endpoint, where we show a Gross-Neveu quantum critical behavior as a function of the relevant coupling strength [26]. As we shall discuss in the following, the mechanism we revealed is reminiscent of the Coleman-Weinberg (CW) theory of mass generation [27, 28].

We solve an interacting BHZ model on a square lattice [1, 2, 24, 29, 30]

$$\mathcal{H} = \sum_{\mathbf{k}} \psi^{\dagger}_{\mathbf{k}} H^{0}_{\mathbf{k}} \psi_{\mathbf{k}} + \sum_{\mathbf{i}} \mathcal{H}^{\mathrm{int}}_{\mathbf{i}} \tag{1}$$

where $\psi_{\mathbf{k}} = [c_{\mathbf{k}1\uparrow}, c_{\mathbf{k}2\uparrow}, c_{\mathbf{k}1\downarrow}, c_{\mathbf{k}2\downarrow}]^{T}$ and the operators $c_{\mathbf{k}\alpha\sigma}$ annihilate an electron with momentum $\mathbf{k}$, orbital

$\alpha = 1, 2$ and spin $\sigma = \uparrow, \downarrow$. If we define $\Gamma_{\mu\nu} = \sigma_\mu \otimes \tau_\nu$ with σ_μ and τ_ν the Pauli matrices, respectively, in the spin and orbital subspaces the single-particle Hamiltonian reads: $H^0_{\mathbf{k}} = [M - 2t(\cos(k_x) + \cos(k_y))]\Gamma_{03} + \lambda \sin(k_x)\Gamma_{31} + \lambda \sin(k_y)\Gamma_{02}$, where $M \geq 0$ is the energy separation between the two orbitals which plays the role of the mass term, t and λ are the intra- and inter-orbital hopping amplitudes. The model is invariant under time-reversal $\mathcal{T}$ and inversion $\mathcal{P}$ symmetries, $U(1)$ spin rotation around the z axis [20, 31–33]. In the following we set our energy unit so that $2t = 1$ and focus on the regime of two electrons per site, i.e. half-filling. The non-interacting model has a continuous topological transition between a QSHI for $M < 2$ and a trivial BI for $M > 2$ through the formation of a gapless Dirac state at $M = 2$ [1].

We assume a generic local interaction which preserves inversion $\mathcal{P}$ and $U(1)$ spin symmetry around the z axis [18, 34]:

$$\mathcal{H}^{int}_{\mathbf{i}} = -\frac{g_N}{2}\hat{N}^2_{\mathbf{i}} - \frac{g_T}{2}\hat{T}^2_{z\mathbf{i}} - \frac{g_S}{2}\hat{S}^2_{z\mathbf{i}} - \frac{g_R}{2}\hat{R}^2_{z\mathbf{i}} \qquad (2)$$

where $\hat{N}_{\mathbf{i}} = \frac{1}{2}\psi^+_{\mathbf{i}}\Gamma_{00}\psi_{\mathbf{i}}$ is half of the total occupation per site, $\hat{T}_{z\mathbf{i}} = \frac{1}{2}\psi^+_{\mathbf{i}}\Gamma_{03}\psi_{\mathbf{i}}$ and $\hat{S}_{z\mathbf{i}} = \frac{1}{2}\psi^+_{\mathbf{i}}\Gamma_{30}\psi_{\mathbf{i}}$ are, respectively, the z component of the orbital polarization and the spin operators and $\hat{R}_{z\mathbf{i}} = \frac{1}{2}\psi^+_{\mathbf{i}}\Gamma_{33}\psi_{\mathbf{i}}$; $\psi_{\mathbf{i}}$ is the Fourier transform of $\psi_{\mathbf{k}}$. In the numerical calculations we will consider $g_N = -(3U - 5J)$, $g_T = U - 5J$, $g_S = U + J$ and $g_R = U - J$ in order to recover the density-density version of the popular Kanamori-Hubbard [35] model used in a variety of works to study the interplay between the Hubbard U and the Hund's exchange J and their effect on TQPTs [24, 36, 37]. We consider non-magnetic solutions in order to study $\mathcal{T}$ symmetry preserving transitions [38, 39]. To simplify the notation in the following we define $\Gamma_{a=N,T,S,R}$ as the set $\frac{1}{2}\Gamma_{\mu\nu=00,03,30,33}$ in order to highlight the different channels.

The starting point of our analysis is to rewrite the partition function of the interacting model (1) in terms of an effective problem coupled to space- and time-dependent (real) bosonic fields $\mathbf{\Delta}_q = \Delta^{a=N,T,S,R}_q$, by performing an Hubbard–Stratonovich transformation. The partition function reads: $\mathcal{Z} \equiv e^{-\beta\mathcal{F}} = \int \mathcal{D}\mathbf{\Delta}\ e^{-\beta\mathcal{N}F[\mathbf{\Delta}]}$ in terms of the free energy functional

$$F[\mathbf{\Delta}] = \sum_{aq}\frac{|\Delta^a_q|^2}{2g_a} - \frac{1}{\beta\mathcal{N}}\mathrm{Tr}\ln(-\mathcal{G}^{-1}_{kq}) \qquad (3)$$

where $q = (\mathbf{q}, i\nu_m)$, $k = (\mathbf{k}, i\omega_n)$, with $\mathbf{q}$, $\mathbf{k}$ wave vectors in the first Brillouin zone and ν_m, ω_n the bosonic and fermionic Matsubara frequencies, respectively, β is the inverse temperature and $\mathcal{N}$ the total number of sites. Tr indicates the trace over momentum, frequency, orbital and spin. Finally $\mathcal{G}_{kq} = \left(i\omega_n + \mu - H^0_{\mathbf{k}}\delta_{\mathbf{k},\mathbf{k}-\mathbf{q}} - V_q\right)^{-1}$ is the interacting one-body Green's function, where $V_q = -\sum_a \Delta^a_q\Gamma_a$ is an effective time-dependent potential depending on $\mathbf{\Delta}_q$.

The natural lowest-order approximation of Eq. (3) is a static mean-field (MF) solution, where the bosonic fields Δ^a_q are approximated with time-independent and spatially uniform quantities. The presence of the mass term breaks explicitly the symmetry between the orbitals, leading to a finite values of the orbital polarization T_z already in the non-interacting model. The non-magnetic solution ($\Delta^S_{MF} = \Delta^R_{MF} = 0$) at half-filling ($\Delta^N_{MF} = 1$), reduces to the single self-consistency equation $\Delta^T = \frac{g_T}{\beta\mathcal{N}}\mathrm{Tr}\,(G^{MF}_k\Gamma_T)$ where $G^{MF}_k = (i\omega_n - H^0_{\mathbf{k}} + \Delta^T\Gamma_T)^{-1}$ is the MF Green's function. Thus, the MF solution simply corrects the mass term M so that the model describes a continuous TQPT occurring at the critical line $M - \frac{1}{2}\Delta^T_{MF} = 2$ [40] as reported in the phase diagram of Fig. 1(b). All along this line the energy gap closes through the formation of a gapless Dirac node at the Γ point as in the non-interacting model. As we show in Fig. 1(a) (dotted line), the orbital polarization smoothly evolves across the topological transition. Coherently with the above scenario, a direct inspection of the MF free energy shows only one minimum for every value of g_T and M.

In this work we overcome the limitations of the MF by approximating the exact free energy functional with a second-order expansion in the fluctuating fields, whose coefficients are variationally determined [41]. We underline that this approach includes effects of higher order beyond the conventional strategy of analyzing Gaussian fluctuations around the MF solution [42]. Most importantly, the expectation values of the fields can change with respect to MF, i.e. $\bar{\mathbf{\Delta}} \neq \bar{\mathbf{\Delta}}_{MF}$. Assuming $\mathbf{\Delta}_q \to \bar{\mathbf{\Delta}} + \mathbf{\Delta}_q$ we can write

$$F[\mathbf{\Delta}] \simeq F^{(2)}[\mathbf{\Delta}] = F[\bar{\mathbf{\Delta}}] + \frac{1}{2}\sum_{abq}\Delta^a_q A^{ab}_q \Delta^b_{-q} \qquad (4)$$

where the variational principle $\mathcal{F} \leq \mathcal{F}^{(2)} + \langle\!\langle F[\mathbf{\Delta}] - F^{(2)}[\mathbf{\Delta}]\rangle\!\rangle$, with $\mathcal{F}^{(2)} = -\frac{1}{\beta}\ln\int\mathcal{D}\mathbf{\Delta}\ e^{-\beta\mathcal{N}F^{(2)}[\mathbf{\Delta}]}$ leads to the new stationary condition $\langle\!\langle\partial_{\Delta^a_q}F[\mathbf{\Delta}]\rangle\!\rangle = 0$ and $A^{ab}_q = \left\langle\!\!\left\langle\partial_{\Delta^a_q}\partial_{\Delta^b_{-q}}F[\mathbf{\Delta}]\right\rangle\!\!\right\rangle$. The symbol $\langle\!\langle\cdot\rangle\!\rangle$ indicates that the averages over the possible configurations are calculated using the second-order probability density of the fluctuating field.

The coefficients A^{ab} in the free energy expansion (4) depend on the averaged dressed Green's function $\langle\!\langle\mathcal{G}_{kq}[\mathbf{\Delta}]\rangle\!\rangle$, which can not be calculated exactly. In order to circumvent this problem we can introduce an auxiliary potential Σ_k implicitly determined by the condition [43, 44]: $\frac{\partial\mathcal{F}^{(2)}}{\partial\Sigma_k} = 0$, which in turn implies that $\langle\!\langle\mathcal{G}_{kq}[\mathbf{\Delta}]\rangle\!\rangle$ coincides with an interacting Green's function in which Σ_k plays the role of a self-energy $G_k = [i\omega_n + \mu - H_0(\mathbf{k}) - \Sigma_k]^{-1}$.

The stationary condition and the expression for A^{ab}_q

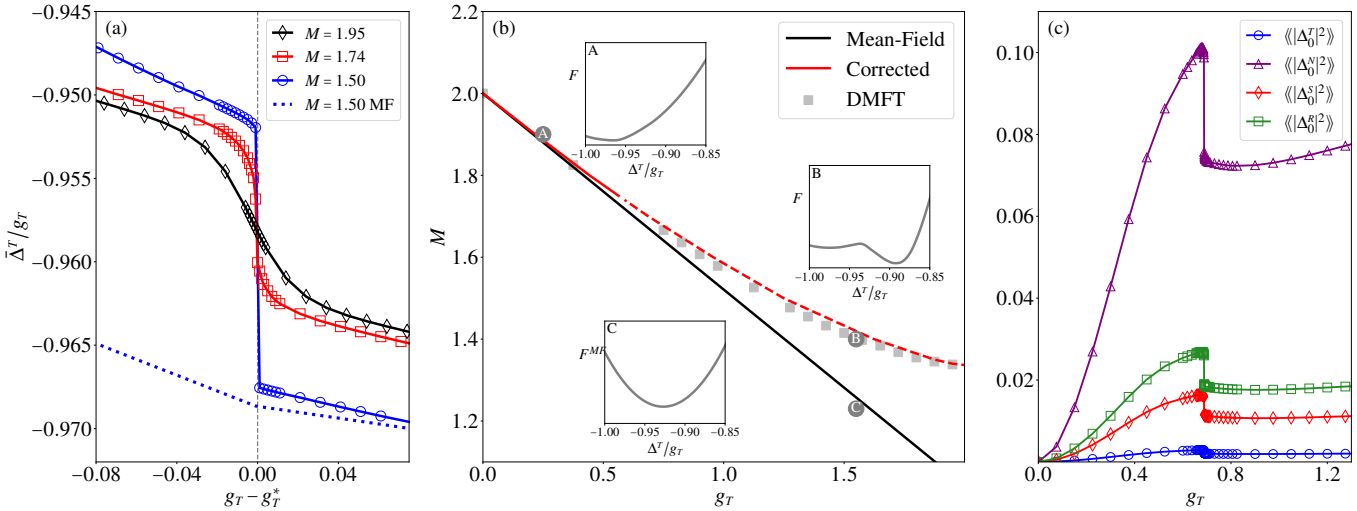

Figure 1. (Color online) (a) Orbital polarization $\bar{\Delta}^T/g_T$ as a function of g_T measured with respect to the TQPT point g_T^*. The open symbols correspond to the fluctuation-corrected results. The dotted line is the MF solution for $M = 1.50$. (b) Phase diagram in the M-g_T plane comparing the topological transition line in the two approximations. The solid lines (black and red) denote a continuous TQPT, while the dashed line (red) marks a discontinuous one. Data from DMFT are indicated with filled symbols (gray). The insets A, B and C show the free energy F as a function of the orbital polarization for the three points marked on the curves. (c) Static and homogeneous components $\langle\langle|\Delta^a_{q=0}|^2\rangle\rangle$ for $a = T, N, S, R$ of the potential fluctuations as a function of g_T across the topological transition for $M = 1.70$.

become

$$\frac{\bar{\Delta}^a}{g_a} = \frac{1}{\beta\mathcal{N}}\mathrm{Tr}\left(G_k\Gamma_a\right);\; A^{ab}_q = \frac{\delta_{ab}}{g_a} - \chi_{ab}(q). \qquad (5)$$

The first expression contains the fluctuation-corrected Green's function, hence it leads to corrected values of the $\bar{\mathbf{\Delta}}$, while the second can be seen as an optimized version of the Random-phase Approximation (RPA), as we shall discuss in the following [42]. Indeed $\chi_{ab}(q) = -\frac{1}{\beta\mathcal{N}}\sum_k \mathrm{Tr}\left[G_k\Gamma_a G_{k+q}\Gamma_b\right]$ is the susceptibility matrix in the space of the different channels which, in presence of odd hybridization between the orbitals, has diagonal structure $\chi_{aa}\delta_{ab}$. Moreover, the symmetries of the interaction ensure that $\chi_{SS} = \chi_{NN}$ and $\chi_{RR} = \chi_{TT}$. Σ_k can be written explicitly up to second order as

$$\Sigma_k = \bar{V} + \sum_{qa} G_{k-q}\left\langle\left\langle|\Delta^a_q|^2\right\rangle\right\rangle \qquad (6)$$

where

$$\left\langle\left\langle|\Delta^a_q|^2\right\rangle\right\rangle = \tfrac{1}{\beta\mathcal{N}}\left[\frac{1}{g_a^{-1} - \chi_{aa}(q)} - g_a\right]. \qquad (7)$$

The diagonal form in the channel index allows us to analyze the contribution of each fluctuating term of the interaction to the potential Σ_k [45]. We emphasize that, formally, the second term in (6) plays the same role of the one-loop quantum correction of the effective Coleman-Weinberg potential [27].

The Eqs.(5) and (6) provide a closed system of non-linear equations for Σ_k and the bosonic fields $\bar{\mathbf{\Delta}}$. Previous studies suggest that the interaction effects on the TQPT are mainly local and that non-local fluctuation play a minor role [46]. Thus, in order to further simplify the treatment in the following we will assume a local $\Sigma_k \simeq \Sigma(i\omega_n)$. We solve this system iteratively using a linear mixing algorithm which typically converges in $10 - 20$ steps. The BZ is discretized with a linear grid of 20×20 points and the Matsubara axis with $L = 8192$ frequencies using an effective inverse temperature $\beta = 500$. The convolution in Eq. (6) is evaluated using a FFT algorithm. We discuss the results obtained for $J/U = 1/8$ and $\lambda = 0.3$.

In Fig.1(a) we show the evolution of the orbital polarization, obtained from the self-consistent value of the bosonic field $\bar{T}_z = \bar{\Delta}^T/g_T$. The behavior at the transition point $g_T^*(M)$ changes qualitatively according to the value of the bare mass M. For a value close to $M = 2$, i.e. the non-interacting transition point, the orbital polarization is continuous with respect to the increasing interaction g_T. This corresponds to a smooth modification of the BI into a non-trivial insulator through the formation of a gapless state at the TQPT. Starting from a farther point, the orbital polarization displays a critical behavior at the transition characterized by a divergent susceptibility $\partial_M \bar{T}_z$. Beyond this point, for any value of M, the orbital polarization is characterized by a discontinuous evolution across the topological transition. This is in stark contrast with the continuous behavior obtained in MF for the same value of the mass, see Fig. 1(a), and

it agrees with previous results obtained via Dynamical Mean-Field Theory (DMFT) [24]. The agreement with DMFT is indeed even quantitative, as shown by the data reported in Fig. 1(b).

These results can be summarised in a phase diagram in the plane g_T-M (see Fig. 1(b)) where we compare the MF and fluctuation-corrected results for the TQPT. The two transition lines remain close for small values of the interaction g_T. Accordingly, the free energy functional F displays a single minimum as a function of Δ^T (inset A in Fig. 1(b)). However, upon increasing the interaction strength the two curves start deviating significantly signalling a crucial impact of the fluctuations.

A direct information about the contribution of the fluctuations in the different channels is reported in Fig. 1(c). The fast increasing behavior with the interaction g_T in all the channels stops at the topological transition towards the QSHI, where these quantities display a discontinuous drop and a successive slow increase. The terms $\langle\langle|\Delta^a_q|^2\rangle\rangle$ enter, through (7), in $\Sigma(i\omega_n)$ giving it a dynamical nature which significantly deviates from its static MF form $\bar{V} = -\bar{\Delta}^T\Gamma_T$. This results in a crucial shift of the self-consistent saddle point value of the bosonic fields. Moreover, as discussed above, while the MF always describes a continuous transition, in the corrected theory the boundary line is continuous up to a critical value g_T^c of the interaction beyond which it becomes of first order. This reflects in the behavior of the free energy near the TQPT point in the intermediate to strong coupling regime, i.e. $g_T > g_T^c$. In the insets B and C of Fig. 1(b) we compare the free energies of a QSHI state near the topological transition for, respectively, the MF and the fluctuation-corrected approximation, where two minima are found: A stable QSHI and a metastable BI.

We thus find that a QCP separates the continuous from the discontinuous regime on the topological transition line, where we also found a divergent orbital susceptibility. Indeed the uniform orbital susceptibility $\mathcal{X}_T = \partial_M \bar{\Delta}^T_{q=0}$ reads, using Eq. (5),

$$\mathcal{X}_T = \frac{-2g_T\chi_{TT}(0)}{1 - g_T\chi_{TT}(0) + \lambda}, \tag{8}$$

which reminds of the RPA result with a correction λ that stems from the implicit dependence of $\Sigma(i\omega_n)$ on the orbital polarization. This quantity also accounts for the contributions of all the other channels of the interaction through the expression of $\Sigma(i\omega_n)$, see Eq. (6) [47]. At the MF level we find $\Sigma(i\omega_n) = -\bar{\Delta}^T\Gamma_T$, so that $\lambda = 0$ and $\mathcal{X}_T$ reduces to the RPA form. For a Hubbard-Kanamori interaction the RPA $\mathcal{X}_T$ diverges only either for negative U or negative M (which lead to different physics), in agreement with the continuous TQPT we always find. Note that this result holds true also when all the coupling constants but g_T vanish and the interaction reduces to $\frac{g_T}{2}\hat{T}_z^2$ [48].

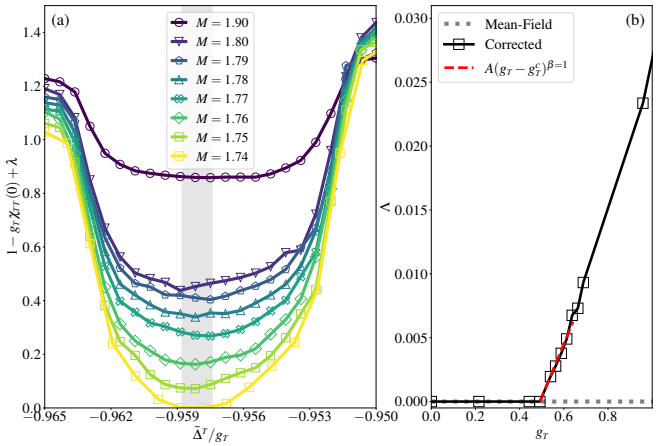

Figure 2. (Color online) (a) The denominator of Eq. (8) as a function of the orbital polarization $\bar{\Delta}^T/g_T$ across the TQPT in the fluctuation-corrected approximation and for different values of the bare mass M. The narrow grey stripe indicates the minimum with its numerical uncertainty. (b) The gap Λ along the TQPT line as a function of the interaction g_T. MF is the dotted grey line, while fluctuation-corrected results are indicated by open symbols and solid line. The (red) dashed line is a linear fit $A(g_T - g_T^c)^{\beta=1}$ ($A \simeq 0.042$) of the critical behavior.

In order to compute λ we consider the zero-frequency limit of $\Sigma(i\omega_n)$ where we obtain $\lambda \simeq \chi_{TT}\partial_{\bar{T}_z}\Lambda$. Since $\partial_{\bar{T}_z}\Lambda < 0$, this correction is negative and tends to enhance $\mathcal{X}_T$. For a fixed value of M the TQPT corresponds to the maximum of the response function which connects the continuous transition to a Widom line [49–51]. The minimum of the denominator in Eq. (8) approaches zero when we reach the QCP, as shown in Fig. 2(a). As we discussed above, in a non-interacting TQPT the spectral gap closes at the transition. We now compute the gap in our scheme from the zero-frequency limit of the self-energy $\Lambda = \mathrm{Re}\Sigma(i\omega_n \to 0) - \bar{V}$. In Fig. 2(b) we report the behavior of Λ at the TQPT as a function of the interaction strength g_T. While in MF the gap is always zero, including the fluctuations we find a finite gap above the QCP ($g_T > g_T^c$). A finite value of the gap Λ corresponds to give a mass to the Dirac fermions at the boundary line. This is consistent with a spontaneous symmetric mass generation process [21–23]. The presence of such finite gap (or mass) makes it impossible to continuously connect the trivial with the non-trivial phase and leads to a first-order TQPT. In addition, we find numerically that the critical behavior near the QCP falls in the Gross-Neveu universality class [22, 26], with an estimated critical exponent $\beta \simeq 1$.

In this work, using a non-perturbative analytical approach to include interactions in the BHZ model, we have demonstrated the crucial role of fluctuations in the different local particle-hole channels to qualitatively change the nature of the TQPT. Within a mean-field the inter-

actions only lead to a renormalization of the bare mass of the model (coupled to the orbital polarization) so that the TQPT has the same character of the non-interacting model. Within our approach the fluctuation contributions change the MF parameters and lead to a discontinuous TQPT for large interactions with a QCP separating the continuous and discontinuous branches. This effect is intrinsically related to a spontaneous gap opening (mass formation) for the otherwise gapless Dirac nodes at TQPT point without any symmetry breaking. The gap follows a Gross-Neveu critical behavior. This process of spontaneous mass generation takes place through a condensed matter analog of the CW mechanism in which one-loop quantum fluctuations lead to a mass without symmetry breaking [27]. We expect that our mechanism can be applied also to other models for topological phase transitions, but also to a wider class of phenomena. A natural example is that of Lifshitz transitions in interacting electronic systems, where the continuous deformation of the Fermi surface topology characteristic of non-interacting systems is expected to share the same destiny of the TQPT, i.e., to become discontinuous for large interactions.

Acknowledgments – F.P. is grateful to P.Coleman and G.Perosa for illuminating discussions specially concerning Ref. [27]. We thank M. Fabrizio, G. Mazza, G. Sangiovanni, J.C. Budich, B. Trauzettel for useful discussions. We acknowledge financial support of MUR via PRIN 2017 (Prot. 20172H2SC4 005), PRIN 2020 (Prot. 2020JLZ52N 002) programs, PRIN 2022 (Prot. 20228YCYY7), National Recovery and Resilience Plan (NRRP) MUR Project No. PE0000023-NQSTI and ICSC–Centro Nazionale di Ricerca in High Performance Computing, Big Data and Quantum Computing, funded by European Union – NextGenerationEU (Grant number CN00000013) - Mission 4 Component 2 Investments 1.3 and 1.4.

[1] B. A. Bernevig, T. L. Hughes, and S.-C. Zhang, Quantum Spin Hall Effect and Topological Phase Transition in HgTe Quantum Wells, Science **314**, 1757 (2006).
[2] X.-L. Qi and S.-C. Zhang, The quantum spin Hall effect and topological insulators, Physics Today **63**, 33 (2010).
[3] J. E. Moore, The birth of topological insulators, Nature **464**, 194 (2010), 10.1038/nature08916.
[4] M. Z. Hasan and C. L. Kane, *Colloquium*: Topological insulators. , Rev. Mod. Phys **82**, 3045 (2010).
[5] B. Bernevig and T. Hughes, *Topological Insulators and Topological Superconductors* (Princeton University Press, 2013).
[6] X.-G. Wen, Colloquium: Zoo of quantum-topological phases of matter, Rev. Mod. Phys. **89**, 041004 (2017).
[7] B. Bradlyn, L. Elcoro, J. Cano, M. G. Vergniory, Z. Wang, C. Felser, M. I. Aroyo, and B. A. Bernevig, Topological quantum chemistry, Nature **547**, 298 (2017).
[8] S. Rachel, Interacting topological insulators: a review, Reports on Progress in Physics **81**, 116501 (2018).
[9] Y. Nambu, Nobel lecture: Spontaneous symmetry breaking in particle physics: A case of cross fertilization, Rev. Mod. Phys. **81**, 1015 (2009).
[10] Y. Zhang, Y. Ran, and A. Vishwanath, Topological insulators in three dimensions from spontaneous symmetry breaking, Phys. Rev. B **79**, 245331 (2009).
[11] S. Y. Zhou, G. H. Gweon, J. Graf, A. V. Fedorov, C. D. Spataru, R. D. Diehl, Y. Kopelevich, D. H. Lee, S. G. Louie, and A. Lanzara, First direct observation of Dirac fermions in graphite, Nat. Phys. **2**, 595 (2006), arXiv:0608069 [cond-mat].
[12] Hsieh D., Qian D., Wray L., Xia Y., Hor Y. S., Cava R. J., and Hasan M. Z., A topological Dirac insulator in a quantum spin Hall phase, Nature **452**, 970 (2008), 10.1038/nature06843.
[13] T. O. Wehling, A. M. Black-Schaffer, and A. V. Balatsky, Dirac materials, Adv. Phys. **63**, 1 (2014), arXiv:1405.5774.
[14] S. M. Young and C. L. Kane, Dirac Semimetals in Two Dimensions, Phys. Rev. Lett. **155**, 126803 (2015).
[15] M. Zahid Hasan, S.-Y. Xu, and M. Neupane, Topological Insulators, Topological Dirac semimetals, Topological Crystalline Insulators, and Topological Kondo Insulators, in *Topol. Insul. Fundam. Perspect.* (Wiley-VCH Verlag, 2015) wiley ed., Chap. 4, pp. 55–100, arXiv:1406.1040.
[16] X.-L. Qi and S.-C. Zhang, Topological insulators and superconductors, Rev. Mod. Phys. **83**, 1057 (2011).
[17] M. Ezawa, Y. Tanaka, and N. Nagaosa, Topological Phase Transition without Gap Closing., Sci. Rep. **3**, 2790 (2013).
[18] S. Rachel, Quantum phase transitions of topological insulators without gap closing, Journal of Physics: Condensed Matter **28**, 405502 (2016).
[19] Y. Jia, P. Wang, C.-L. Chiu, Z. Song, G. Yu, B. Jäck, S. Lei, S. Klemenz, F. A. Cevallos, M. Onyszczak, N. Fishchenko, X. Liu, G. Farahi, F. Xie, Y. Xu, K. Watanabe, T. Taniguchi, B. A. Bernevig, R. J. Cava, L. M. Schoop, A. Yazdani, and S. Wu, Evidence for a monolayer excitonic insulator, Nature Physics **18**, 87 (2022).
[20] A. Amaricci, G. Mazza, M. Capone, and M. Fabrizio, Exciton condensation in strongly correlated quantum spin hall insulators, Phys. Rev. B **107**, 115117 (2023).
[21] Y.-Z. You, Y.-C. He, C. Xu, and A. Vishwanath, Symmetric fermion mass generation as deconfined quantum criticality, Phys. Rev. X **8**, 011026 (2018).
[22] K. Slagle, Y.-Z. You, and C. Xu, Exotic quantum phase transitions of strongly interacting topological insulators, Phys. Rev. B **91**, 115121 (2015).
[23] J. Wang and Y.-Z. You, Symmetric mass generation, Symmetry **14**, 10.3390/sym14071475 (2022).
[24] A. Amaricci, J. C. Budich, M. Capone, B. Trauzettel, and G. Sangiovanni, First-order character and observable signatures of topological quantum phase transitions, Phys. Rev. Lett. **114**, 185701 (2015).
[25] Y. Yamaji, T. Misawa, and M. Imada, Quantum criticalities induced by lifshitz transitions, Journal of Magnetism and Magnetic Materials **310**, 838 (2007), proceedings of the 17th International Conference on Magnetism.
[26] Y. Liu, Z. Wang, T. Sato, W. Guo, and F. F. Assaad, Gross-neveu heisenberg criticality: Dynamical generation of quantum spin hall masses, Physical Review B **104**,

10.1103/physrevb.104.035107 (2021).
[27] S. Coleman and E. Weinberg, Radiative corrections as the origin of spontaneous symmetry breaking, Phys. Rev. D **7**, 1888 (1973).
[28] J. G. Rau, P. A. McClarty, and R. Moessner, Pseudo-goldstone gaps and order-by-quantum disorder in frustrated magnets, Phys. Rev. Lett. **121**, 237201 (2018).
[29] C. Wu, B. A. Bernevig, and S.-C. Zhang, Helical liquid and the edge of quantum spin hall systems, Phys. Rev. Lett. **96**, 106401 (2006).
[30] X. Qian, J. Liu, L. Fu, and J. Li, Quantum spin hall effect in two-dimensional transition metal dichalcogenides, Science **346**, 1344 (2014).
[31] A. Blason and M. Fabrizio, Exciton topology and condensation in a model quantum spin hall insulator, Phys. Rev. B **102**, 035146 (2020).
[32] J. C. Budich, B. Trauzettel, and P. Michetti, Time reversal symmetric topological exciton condensate in bilayer hgte quantum wells, Phys. Rev. Lett. **112**, 146405 (2014).
[33] G. Mazza, M. Rösner, L. Windgätter, S. Latini, H. Hübener, A. J. Millis, A. Rubio, and A. Georges, Nature of symmetry breaking at the excitonic insulator transition: ta_2nise_5, Phys. Rev. Lett. **124**, 197601 (2020).
[34] M. Hohenadler and F. F. Assaad, Correlation effects in two-dimensional topological insulators, Journal of Physics: Condensed Matter **25**, 143201 (2013).
[35] A. Georges, L. de' Medici, and J. Mravlje, Strong Correlations from Hund's Coupling., Annu. Rev. Condens. Matter Phys. **45**, 137 (2013).
[36] P. Werner and A. J. Millis, High-Spin to Low-Spin and Orbital Polarization Transitions in Multiorbital Mott Systems, Phys. Rev. Lett. **99**, 126405 (2007).
[37] J. C. Budich, R. Thomale, G. Li, M. Laubach, and S.-C. Zhang, Fluctuation-induced topological quantum phase transitions in quantum spin-Hall and anomalous-Hall insulators, Phys. Rev. B **86**, 201407 (2012).
[38] A. Amaricci, J. C. Budich, M. Capone, B. Trauzettel, and G. Sangiovanni, Strong correlation effects on topological quantum phase transitions in three dimensions, Phys. Rev. B **93**, 235112 (2016).
[39] A. Amaricci, L. Privitera, F. Petocchi, M. Capone, G. Sangiovanni, and B. Trauzettel, Edge state reconstruction from strong correlations in quantum spin hall insulators, Phys. Rev. B **95**, 205120 (2017).
[40] In this work we consider values of the interaction which do not lead to a change of sign in the renormalized mass term.
[41] J. A. Hertz and M. A. Klenin, Fluctuations in itinerant-electron paramagnets, Phys. Rev. B **10**, 1084 (1974).
[42] Y. Klein, M. Casula, D. Santos-Cottin, A. Audouard, D. Vignolles, G. Fève, V. Freulon, B. Plaçais, M. Verseils, H. Yang, L. Paulatto, and A. Gauzzi, Importance of non-local electron correlation in the BaNiS2 semimetal from quantum oscillations studies, Phys. Rev. B **97**, 075140 (2018).
[43] Y. Kakehashi, Dynamical coherent-potential approximation to the magnetism in a correlated electron system, Phys. Rev. B **65**, 184420 (2002).
[44] N. B. Melnikov, B. I. Reser, and V. I. Grebennikov, Extended dynamic spin-fluctuation theory of metallic magnetism, Journal of Physics: Condensed Matter **23**, 276003 (2011).
[45] O. Gunnarsson, T. Schäfer, J. LeBlanc, E. Gull, J. Merino, G. Sangiovanni, G. Rohringer, and A. Toschi, Fluctuation diagnostics of the electron self-energy: Origin of the pseudogap physics, Physical Review Letters **114**, 10.1103/physrevlett.114.236402 (2015).
[46] L. Crippa, A. Amaricci, S. Adler, G. Sangiovanni, and M. Capone, Local versus nonlocal correlation effects in interacting quantum spin hall insulators, Phys. Rev. B **104**, 235117 (2021).
[47] L. Fanfarillo, L. Benfatto, and C. Castellani, Current-current fermi-liquid corrections to the superconducting fluctuations on conductivity and diamagnetism, Phys. Rev. B **85**, 024507 (2012).
[48] B. Roy, P. Goswami, and J. D. Sau, Continuous and discontinuous topological quantum phase transitions, Phys. Rev. B **94**, 041101 (2016).
[49] L. Xu, P. Kumar, S. V. Buldyrev, S.-H. Chen, P. H. Poole, F. Sciortino, and H. E. Stanley, Relation between the widom line and the dynamic crossover in systems with a liquid–liquid phase transition, Proceedings of the National Academy of Sciences **102**, 16558 (2005), https://www.pnas.org/doi/pdf/10.1073/pnas.0507870102.
[50] G. G. Simeoni, T. Bryk, F. A. Gorelli, M. Krisch, G. Ruocco, M. Santoro, and T. Scopigno, The widom line as the crossover between liquid-like and gas-like behaviour in supercritical fluids, Nature Physics **6**, 503 (2010).
[51] G. Sordi, P. Sémon, K. Haule, and A. M. S. Tremblay, Pseudogap temperature as a widom line in doped mott insulators, Scientific Reports **2**, 547 (2012).